Available at
www.ElsevierComputerScience.com
POWERED BY SCIENCE DIRECT®

Signal Processing 85 (2005) 2190–2212

SIGNAL PROCESSING

www.elsevier.com/locate/sigpro

Nonstationary nature of the brain activity as revealed by EEG/MEG: Methodological, practical and conceptual challenges

Alexander Ya. Kaplan[a,*], Andrew A. Fingelkurts[b,c,**], Alexander A. Fingelkurts[b,c], Sergei V. Borisov[a,d], Boris S. Darkhovsky[e]

[a]*Human Brain Research Group, Biological Faculty, Moscow State University, Moscow, Russian Federation*
[b]*BM-SCIENCE– Brain and Mind Technologies Research Centre, P.O. Box 77, FI-02601, Espoo, Finland*
[c]*BioMag Laboratory, Engineering Centre, Helsinki University Central Hospital, P.O. Box 442 FIN-00290 Helsinki, Finland*
[d]*Laboratory of Computer and Information Science, Neural Networks Research Centre, Helsinki University of Technology, Finland*
[e]*Institute for System Analysis Russian Academy of Sciences, Prosp. 60 Let Oktyabrya 9, Moscow, 117312, Russian Federation*

Available online 28 July 2005

Abstract

Revealing the functional meaning of EEG and MEG signals' nonstationarity and metastability is one of the major topics in current brain research. Indeed, the explicit quasi-stationary phenomena in the activity of large neuronal populations are still largely unknown. However, the fast dynamics of quasi-stationary episodes in EEG/MEG signal, together with rapid transitive periods between them, fit to the time scale of our conscious experience on the one hand, and to the theory of coupled nonlinear dynamical subsystems on the other hand. The global integrity of local quasi-stationary states of EEG/MEG signal is the other side of metastable brain dynamics. In the current review paper we present methodologies for studying the quasi-stationary composition of both local EEGs/MEGs and the inherent synchrony between quasi-stationary structures in pairs of EEG/MEG channels. To obtain quantitative characteristics of segmental organization and structural synchrony of multichannel EEG/MEG signal, the original algorithms and program tools have been used. Convincing results obtained for the experimental models and simulated data are presented and discussed in detail. A novel framework for the analysis of EEG/MEG time series that alternate between different operating modes is suggested.

Keywords: MEG/EEG; Nonstationary processes; Quasi-stationarity segments; Structural synchrony; Alpha rhythm; Microstates; Metastability; Cognitive functions; Brain

*Corresponding author. Human Brain Research Group, Biological Faculty, Moscow State University, 119992 Moscow, Russian Federation.

**Corresponding author. BM-SCIENCE–Brain & Mind Technologies Research Centre, P.O. Box 77, FI-02601, Espoo, Finland. Fax: +358 9 541 4507.

E-mail addresses: akaplan@mail.ru (A.Ya. Kaplan), andrew.fingelkurts@bm-science.com (A.A. Fingelkurts).

0165-1684/$ - see front matter © 2005 Elsevier B.V. All rights reserved.
doi:10.1016/j.sigpro.2005.07.010

1. Introduction

> Its 〈EEG〉 full potential can now be utilized since recording technology and computational power for the large data masses has become affordable. However, basic traditional strategies in EEG need reviewing.
> Lehmann D. In: Psychophysiol. 1 (1984) 267–276 [68].

The search to understand how human beings create intentional behavior and how the mental world emerges within the human brain on the basis of neuronal activity, inevitably leads researchers to study neuronal nets co-operation. The neuron doctrine in its classical mode has served well as the theoretical basis for the great advances in the current understanding of how the human brain works [1]. However, the behavior of many billions of neurons organized in the noisy networks cannot be explained using only the knowledge of its basic properties obtained from that neuronal microscopic level [2,3]. As a consequence, a global brain dynamics emerged at the large-scale level from the cooperative interactions among widely distributed, densely interconnected and continuously active neurons has been postulated ([4,5] just to mention a few).

Here the principal question arises, however: what are the mechanisms in the human brain that underlie functional cooperation of such large-scale and continuously changing neural populations, consisting of billions of neurons? Modern theoretical and experimental work suggests that the assemblies of coupled and synchronously active neurons represent the most plausible candidates for the understanding of brain dynamics [6–8]. The majority of the neuronal assemblies are nonlinear excitable systems. Thus, it becomes common to apply principles derived from nonlinear dynamics to characterize these neuronal systems [8,9]. One of the fundamental predictions from this framework is that self-organization depends on the appearance of sudden, macroscopic transitions between relatively stable states of a complex system [8,10]. Therefore, the presence of transitions between metastable patterns of brain activity could be considered as the basic operational architecture of the brain and also as a manifestation of the dynamic repertoire of the brain functional states [4,11–14]. The most explicit example of the cooperated neuronal activity is the well-known EEG/MEG oscillations [15–17].

From the early electrophysiological studies, it has been shown that large-scale patterns of synchronized neuronal activity (or EEG/MEG) are ever changing and thus exhibit a considerable variability over time. Therefore, until now, analysis of the EEG/MEG signal has been based mainly on statistical data processing in order to obtain the stable and reliable characteristics. The key assumption underlying such statistical analyses is the "*stationarity*" of the registered signal. Usually, manifestations of *non*stationarity in the real EEG/MEG signal are either carefully eliminated, or are considered as an unavoidable "noise" in the system. To minimize this so-called "noise", various procedures of smoothing and averaging are applied to the data. Even though these approaches have revealed many important characteristics of the signal (for example, the functional significance of different EEG/MEG frequency bands; [15,16]), the initially high time-resolution of the signal is usually lost under such conditions. In the meantime, it is obvious that regardless of how powerful or statistically significant the different estimations of averaged EEG/MEG characteristics may be, there might be difficulties in arriving at a meaningful interpretation of these if they are not matched to their inherent piecewise stationary structure [18–20].

It now appears that the practice of analyzing EEG/MEG signals based on the assumption of stationarity and using the "timeless" methods is coming to an end, slowly being superceded by a new paradigm based on the opposite assumption: that the brain activity is essentially *nonstationary* [14]. Here another important question arises: does this mean that neuroscientists should employ the phenomenon of "*nonstationarity*" in a quest for new clues about the brain functioning? Based on our research, we believe that the basic source of the observed nonstationarity in EEG/MEG signal is not due to the casual influences of the external stimuli on the brain mechanisms, but rather it is a reflection of switching of the inherent metastable states of neural assemblies during brain

functioning. At the EEG/MEG level the moments of switching are reflected in a sequence of abrupt transitive processes which make up the EEG/MEG segments [21,22]. In this case, the time dynamics of such switching can be considered as a kind of "leitmotiv" which determines the coordinated participation of many neural ensembles in harmonious brain activity (for the reviews, see [12,14,21,23]).

The issue of segmental description of brain activity has been addressed by several researchers (see review [24]); however, the most successful attempt was made by analyzing and comparing the spatial configurations of the momentary electric brain field. Thus, it has been shown that an EEG consists of sub-second duration epochs with a stable spatial configuration (microstates) lasting about 100–200 ms and separated by rapid topographical changes [25]. However, because this segmental methodology is based on momentary brain electric field configurations, it does not provide information about frequency domain. In such a case the relationship between microstates and frequency oscillations remains unclear. Another drawback of this method concerns the involvement of different cortical areas: even though a spatial segmentation of multichannel EEG/MEG is a very important approach for studying the quasi-stationary structure of brain activity, it is, however, lacking of the time-dimensional information in each cortical area separately. A crucial step to overcome these limitations is an approach firstly suggested by Bodenstain and Praetorius [26]. They suggested to segment the individual EEG channel by means of autoregression modeling. Several other segmentation techniques for the individual EEG/MEG channels have also been used intensively ([24,27] just to mention a few), mainly utilizing parametric approaches. However, all parametrical approaches are initially "defective" because they have inherent limitations when applied to the analysis of EEG/MEG signal; the most significant one is the absence of a universal EEG (or MEG) mathematical model (for a detail discussion, see [28]).

To overcome the limitations of these methods, we have introduced the nonparametric approach for EEG segmentation which does not use any analytical models, but rather searches (based only on statistical evaluation) for the switching between quasi-stationary segments in the EEG/MEG signal [22,29]. In the current version (SECTION 01®), this technology enables the characterization of each channel in multichannel EEG/MEG as a set/sequence of segments with certain attributes [30]. However, the knowledge about the dynamic metastability of brain activity would be incomplete without studying the spatial distribution of EEG/MEG segments along the cortex. To assess the spatial domain, a methodology to estimate a new kind of synchrony in the multichannel EEG/MEG signal (called *structural synchrony*) has been developed (JUMPSYN 01® algorithm). The Structural Synchrony Index measures the coincidence level between the switching moments (boundaries between segments) between different EEG/MEG channels [31]. A detailed description of the current versions of both technologies is presented below in this paper.

The aim of the present review paper is therefore multifold: (1) To present and observe the new, integrated methodological approaches for detecting quasi-stationary EEG/MEG segments and their synchrony between different EEG/MEG locations; (2) to observe the modeling and experimental data; and (3) to undertake a conceptual analysis of data in the framework of metastable concept of brain dynamics ([13]; for a recent review see [4,12]).

2. Methods

2.1. Nonparametric adaptive level segmentation of EEG/MEG

Before describing the main steps of this approach, we explain how changes in probabilistic characteristics in the EEG/MEG can be formally defined. It has been assumed that an observed piecewise stationary process like EEG/MEG is "glued" from several quasi-stationary processes [29,32]. Thus, the task is to divide the signal into quasi-stationary segments by estimating these points of "gluing". These instants within short-time window, when the EEG/MEG amplitude is

changed abruptly, are identified as *rapid transition processes* (RTP). RTP is supposed to be of minor length, and therefore can be treated as a point or near-point. It was proved that amplitude variability is indeed the main contributor to temporal modulation of the variance and power of the signal under investigation [33].

The adaptive *non*parametric EEG/MEG segmentation method (SECTION 01®, Human Brain Research Group, Moscow State University) was performed in two stages (Fig. 1A). This method does not build any mathematical model of the signal with defined parameters and for the search of the stationary segments in the signal it compares the statistics of stochastic amplitude distributions before and after of preliminary RTP. The first stage was performed in two steps. During the *first* step, the native EEG/MEG values were converted into the absolute values (module), since only envelop of the signal is used in the following step (Hilbert transform can also be used to provide envelope estimates). *Second* step corresponds to the basic procedure of segmentation: The main idea is in comparison of the ongoing EEG/MEG amplitude absolute values averaged in the sliding *test*-window and in the sliding *level*-window (test window $\ll$ level window). All amplitude values in the windows are weighted equally. The duration of windows is short (6–800 ms) and dependent on the analyzed frequency range and sampling rate of the signal; the shift of both windows is equal to one data-point. The use of short time windows is motivated by the need for tracking nonstationary transient cortical processes on a sub-second time scale. As a result of averaging in sliding test- and level-windows, two new sequences (test-*t* and level-*l*) constructed from the initial one, and placed on the same time-scale (Fig. 1A). The time-instants corresponding to the crossing of *t*- and *l*-time-series become the preliminary estimate of RTPs.

To estimate the statistically significant RTPs the two conditions should meet (Fig. 1B). First condition estimates the steepness of a change (Fig. 1B and a): the EEG/MEG amplitude values are averaged at the *t*-time-series within *n* data-points before (M_{-n}) and after (M_{+n}) a preliminary RTP. If the result of subtraction ($M_{+n}-M_{-n}$) is statistically significant (the Student criteria, $p<0.05$ with coefficient 0.3), then this first condition is accepted and second condition should be tested. Second condition (Fig. 1B and b) must be fulfilled in order to eliminate possible "false alerts" associated with anomalous brief peaks in the EEG/MEG amplitude. Consecutive five points of the digitized EEG/MEG following this preliminary RTP must have a statistically significant difference between averaged amplitude values in the *t*- and *l*-time-series (the Student criteria, $p<0.05$ with coefficient 0.1). Only if these two criteria are met, the preliminary RTPs are assumed as actual. With this technique, the sequence of RTPs with statistically proven ($p<0.05$, Student *t*-test) time coordinates has been determined for each EEG/MEG location individually for each 1-min epoch. By varying the parameters of this technique it is possible to obtain the segments corresponding to a more or less detailed structure of the EEG/MEG. Therefore, there are prospects for the description of the structural EEG/MEG organization as a hierarchy of segmental descriptions on different time scales [22].

After quasi-stationary segments (indexed by RTP) were obtained, several characteristics (attributes) of segments can be calculated (separately for each channel):

1. Average amplitude (A) within each segment (μV^2)—as generally agreed, indicates mainly the volume or size of neuronal population: indeed, the more neurons recruited into assembly through local synchronization of their activity, the higher will be the amplitude of corresponding to this assembly oscillations in the EEG/MEG [17].
2. Average length (L) of segments (ms)—illustrates the functional life span of neuronal population or the duration of operations produced by this population: since the transient neuronal assembly function during particular time interval, this period is reflected in EEG/MEG as a stabilized interval of the quasi-stationary activity [23].
3. Coefficient of amplitude variability (V) within segments (%)—shows naturally the stability of local neuronal synchronization within neuronal population or assembly.

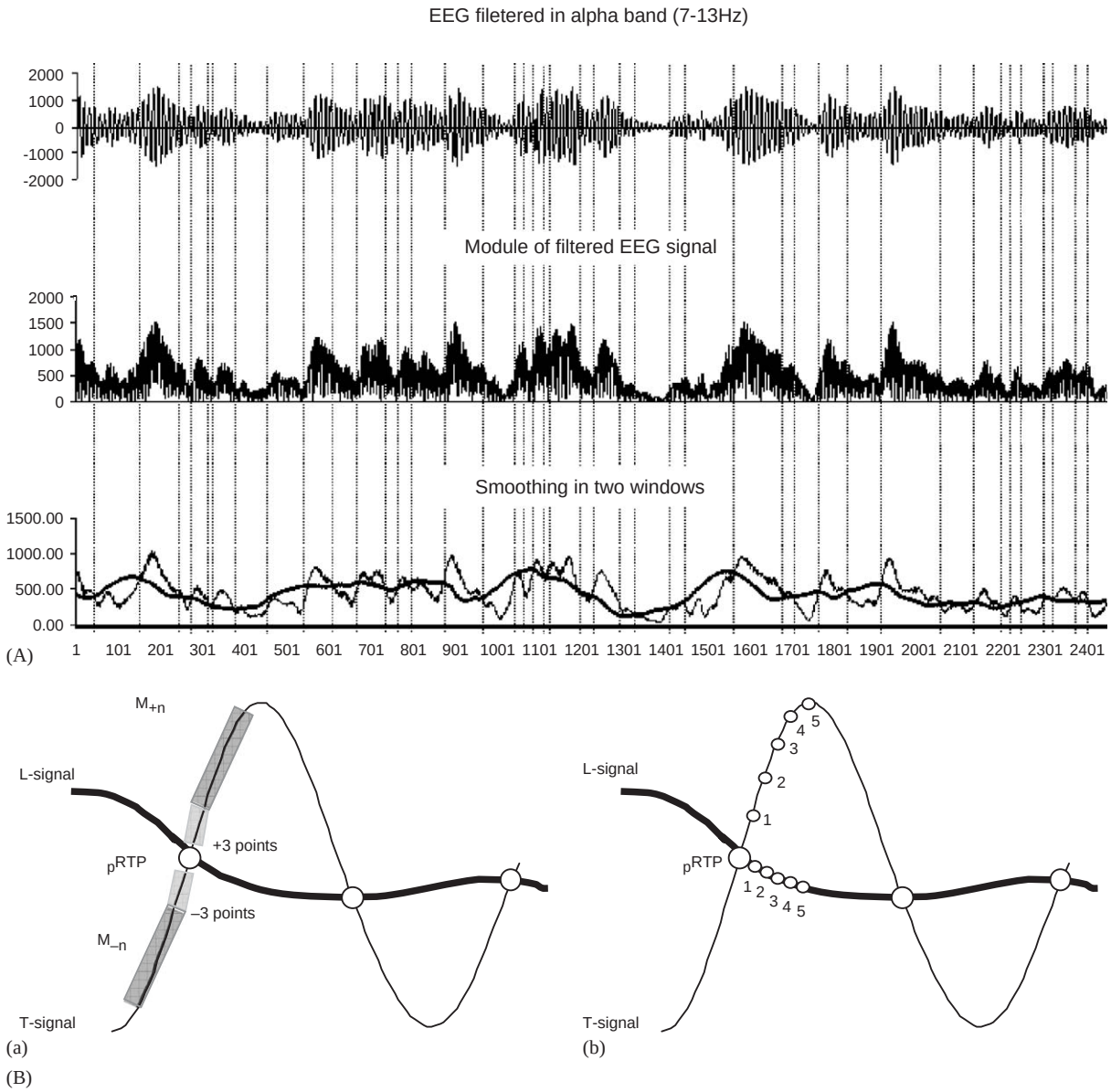

Fig. 1. Nonparametric adaptive level segmentation of EEG/MEG (schematic presentation). *A*, stages of segmentation. On the horizontal axis the data-points of digitized signal is shown. On the vertical axis the amplitude of the signal is shown in μV^2. Vertical dotted lines indicate the time coordinates of preliminary RTPs. *B*, two conditions for estimation the statistical significance of preliminary RTP (pRTP). Explanation in the text.

4. Average amplitude relation (*AR*) among adjacent segments (%)—indicates the neuronal assembly behavior—growth (recruiting of new neurons) or distraction (functional elimination of neurons) [34].
5. Average steepness (*S*) among adjacent segments (estimated in the close area of RTP) (%)—reflects the speed of neuronal population growth or functional distraction [30].

The comparison of the same segment attributes between different experimental conditions or functional states was performed using Wilcoxon matched pairs *t*-test.

2.2. Calculation of the structural synchrony index

The next step was to estimate the synchronization of rapid transition processes (RTP) in EEG/MEG among different cortical areas through the index of EEG/MEG structural synchrony (ISS). Traditionally coherence and correlation has been the main methods to assess the degree of synchronization between brain signals [35]. It is interesting that initial idea, advocating the correlation approaches as an attempt to quantitatively describe the relationship in the activity of cortical areas, has gradually transformed into the postulation of the presence of an "interrelation" between different sections of the brain only in the case of a high significance of crosscorrelation and coherency. However, in a strict sense, the coherence value indicates only the linear statistical link between EEG/MEG curves in a frequency band. Meanwhile, it is obvious that in general the absence of similar types of statistical relation between two processes does not mean the absence of any interaction between them at all (for critical discussion see [31,36]. John C. Show and David Simpson also stressed that one must be careful about interpreting coherence (and partial coherence) as an indicator of functional connectivity [37] and pointed out that EEG signals may show a finite correlation even when recorded from separate subjects [38]. Recently several new methods for detecting functional connectivity between cortical areas have been published: partial directed coherence [39], dynamic imaging of coherent sources [40], structural equation models for fMRI [41], and phase synchrony [42]. However, all these methods have several serious limitations (for a discussion, see [43]).

The ISS index (JUMPSYN 01®, Human Brain Research Group, Moscow State University), overcome the disadvantages of conventional methods, and can reveal inherent functional interrelationships of cortical areas different from those measured by correlation, coherence and phase analysis (for a discussion, see [43]).

The technology for ISS estimation was as follows. Each RTP in the *reference* EEG/MEG channel (the channel with the minimal number of RTPs from any pair of EEG/MEG channels) was surrounded by a short "window" (ms). It was taken that any RTP from another (*test*) EEG/MEG channel coincided if it fell within this window. Formally the ISS was computed as follows:

$$\mathrm{ISS} = m_{\mathrm{windows}} - m_{\mathrm{residual}},$$

where $m_{\mathrm{windows}} = 100 * sn_{\mathrm{w}}/sl_{\mathrm{w}}$; $m_{\mathrm{residual}} = 100 * sn_{\mathrm{r}}/sl_{\mathrm{r}}$; sn_{w} the total number of RTPs in all windows (window for synchronization) in the test channel; sl_{w} the total length of EEG/MEG recording (in data points) inside all windows in the test channel; sn_{r} the total number of RTPs outside the windows (window for synchronization) in the test channel; sl_{r} the total length of EEG/MEG recording (in data points) outside the windows in the test channel.

It is obvious, however, that even in the absence of any functional cortical interregional cooperation there should be a certain stochastic level of RTPs coupling, which would reflect merely occasional combinations. The values of such stochastic inter-area relations should be uniform and substantially lower than in the actual presence of functional interrelation between areas of EEG/MEG channels. Thus, to arrive at a direct estimation of a 5% level of statistical significance of the ISS ($p < 0.05$), computer simulation of RTPs synchronization was undertaken based on random shuffling of time segments marked by RTPs (500 independent trials). These share the properties of the experimental data (number of RTPs in each EEG/MEG channel of analyzed pair, number of segments, and number of windows of synchronization), but the time coordinates of RTPs were altered randomly in each trial so as to destroy the natural temporal structure of the data. Justification for this approach can be found in [44]. However, other approaches are also possible (see for example [45]).

As a result of 500 times repeated random reshuffling of the time segments marked by RTPs

the stochastic level of RTPs coupling (ISS_{stoh}), and the upper and lower thresholds of ISS_{stoh} significance (5%) were calculated. These values represent an estimation of the maximum (by module) possible stochastic rate of RTPs coupling (confidence levels). Thus, only those values of ISS which exceeded the upper (active coupling) and lower (active decoupling) thresholds of ISS_{stoh} have been assumed to be statistically valid ($p<0.05$). Thus, the ISS tends towards zero where there is no synchronization between the EEG/MEG segments and has positive or negative values where such synchronization exists. Positive values indicate 'active' *coupling* of EEG/MEG segments (synchronization of EEG/MEG segments are observed significantly more often than expected by chance), whereas negative values mark 'active' *decoupling* of segments (synchronization of EEG/MEG segments are observed significantly less than expected by chance). From a qualitative perspective, the (de)coupling of EEG/MEG segments corresponds to the phenomenon of synchronization of brain operations or Operational Synchrony, OS (for review, see [21,23]).

2.3. EEG/MEG registration

All EEG recordings were performed in an electrically and magnetically shielded room in Human Brain Research Group, Moscow State University and in the BioMag Laboratory, Helsinki University Central Hospital. EEGs were recorded with 16- and 60-channel data acquisition systems with a frequency band of 0.03–30 Hz (sampling rate 128 Hz). Different montages were used (specified in the Results and Discussion section). The link ears-lobe electrodes were used as reference. The impedance of the recording electrodes was always below 5 kΩ. Vertical and horizontal electro-oculograms were recorded.

MEG was recorded continuously in a magnetically shielded room with a 306-channel whole-head device in the Low Temperature Laboratory at the Helsinki University of Technology (Neuromag Vectorview, Helsinki, Finland). The sensor elements of the device comprise two orthogonal planar gradiometers and one magnetometer. The data was digitized at 300 Hz. The passband filter of the MEG recordings was 0.06–100 Hz. Only subset of these 306 channels was used (specified in the Results and Discussion section).

EEG/MEG epochs containing artifacts due to eye blinks, significant muscle activity or movements were automatically rejected. The presence of an adequate signal was also determined by visually checking of the each raw signal on the computer screen after automatic artifact rejection.

3. Results and discussion

In the present work we examined the new methodological approaches for EEG/MEG signal analysis in several modeling experiments. We used native EEG/MEG signal as well as filtered in alpha (7–13 Hz) and beta (15–21 Hz) frequency bands, as well as surrogate EEG/MEG data. Using surrogate data we approached the relative rate of stochastic alternations (confidence levels) of our estimations in the actual EEG/MEG.

3.1. Adaptive EEG segmentation

This part of the work was focused on the analysis of the dynamics of functional neuronal assembles (or populations). Neuronal assembly usually is described as a group of neurons or neural masses for which correlated activity persists over substantial time intervals [17] and underlies basic operations of informational processing [30]. At the level of EEG (and MEG) these intervals should be reflected in the periods of quasi-stationary activity that operates in different frequency ranges (for the review see [21]). Such segments of quasi-stationarity were obtained using segmentation approach (see Section 2). Rapid transition processes (RTP) in EEG amplitude in such a way are, in fact, the markers of boundaries between quasi-stationary segments. This approach focuses on the local processes in the cortex and thus permits assessing the mesolevel description of cortex interactions (interactions within transient neuronal assemblies) through large-scale estimates [34].

Fig. 2 illustrates the typical example of automatic detection of RTPs in 16-channel spontaneous

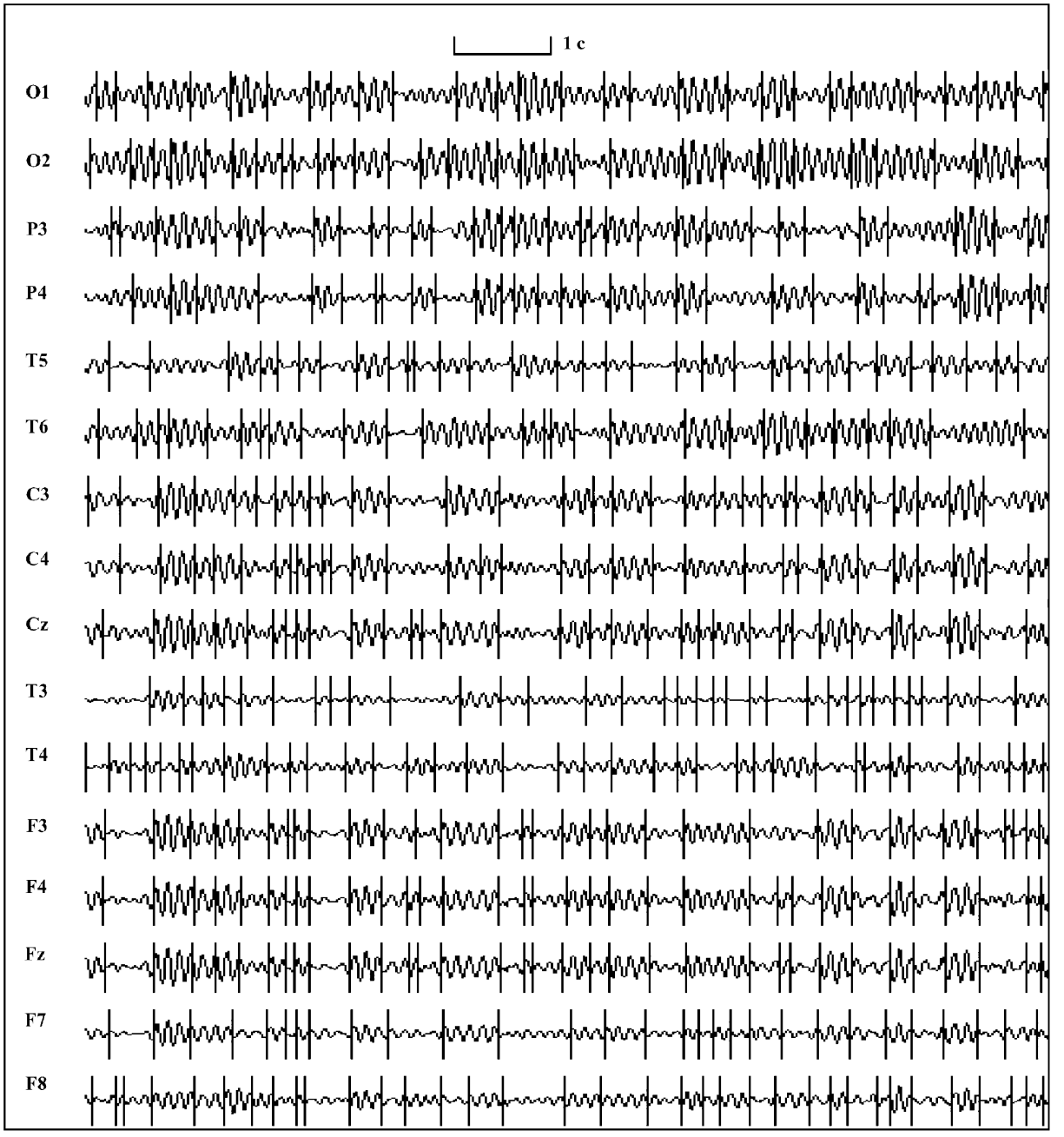

Fig. 2. Typical example of 16-channel spontaneous EEG record (filtered in alpha frequency band: 7–13 Hz) with automatically detected rapid transition processes (RTP). Figure modified from Fingelkurts and Fingelkurts, 2001 Brain and Mind.

EEG recording filtering in the alpha frequency band (7–13 Hz). As it seen from the figure, RTPs mark not only the periods of presence or absence of alpha-spindles, but also the phasic changes of it independently from the power of alpha rhythm.

The majority of quasi-stationary segments have had a duration less than 1 s (Fig. 2). The same finding was obtained consistently in the number of experimental settings [31,34,44,46–49]. For each 1-min EEG recording ($n = 80$, male healthy subjects, rest condition, closed eyes) about 200–270 segments for alpha activity and 240–280 segments for beta activity were found. However, the specific proportions of the duration and the number of stationary segments strongly vary between different cortical areas and depended on the stage of cognitive task (data not shown, see [31,47]). These findings suggest a functional significance of segmental EEG architectonics during both spontaneous (stimulus independent) and induced (stimulus dependent) brain activity.

If the majority of RTPs are really the markers of the boundaries of quasi-stationary EEG/MEG segments, then the coefficient of within-segment amplitude variability (V) should be substantially higher for the randomly (stochastically) altered EEG/MEG when compared with actual one. As an example the analysis of EEG data ($n = 10$) was provided. In order to find the V value of the stochastic alternation in the actual EEG, it was subjected to a randomized mixing of all consequent amplitude values within each EEG channel separately. In such a way, the natural dynamics of amplitude values sequence within each EEG channel were completely destroyed, but the average values of amplitude for each channel remained the same as before mixing. This modified EEG was described as "random". Using the procedure of randomly mixing amplitude values, the relative values of the V for stochastic alternations was estimated for each channel (Fig. 3).

The V values of the actual EEG substantially differed ($p < 0.01 - p < 0.001$) from the "random" EEG. An excessive increase in the V values up to 50–60% for "random" EEG may indicate a stochastic process (compare with 20–30% for the actual EEG). This value presents an estimation of the maximum possible rate of relative alteration in the amplitude variability for a given EEG. Thus, this estimation testifies the fact that obtained segments in the actual EEG really have quasi-stationary nature and reflect the episodes of relative stabilization of neuronal activity within

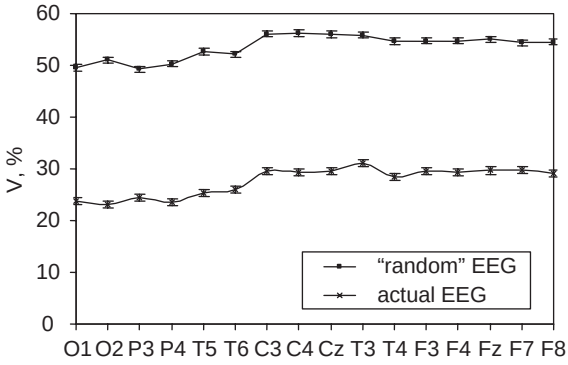

Fig. 3. Averaged ($n = 10$, resting condition, closed eyes) values of the coefficient of amplitude variability (V) for alpha activity within quasi-stationary EEG segments. For comparisons analogous V values are shown for the same randomized EEG.

separate neuronal assemblies. One may notice also that occipital and temporal EEG locations exhibited more stationary segments ($p < 0.05$) than central and frontal locations (Fig. 3).

These findings were characteristic for subjects with well-developed alpha activity. In order to check the behavior of segments in the EEG with a weak alpha rhythm we used the data obtained from the healthy subject with so-called "flat" EEG. Fig. 4 presents as an example the distributions of average amplitude (A) and length (L) values of segments obtained for the subject with a high alpha activity and the subject with a "flat" EEG ($n = 10$ for each subject) during rest condition with closed eyes. EEGs of both subjects were filtered in the alpha frequency band (7–13 Hz).

Even with the absence of alpha-peak in the EEG power spectrum ("flat" EEG), segmentation analysis reveled notably wide distribution of A values. However, the vast majority of segments in the "flat" EEG were characterized by lower amplitudes when compared with the "high-alpha" EEG (Fig. 4). The L values were also lower in the "flat" EEG than in the "high-alpha" EEG. Analogous data were obtained for MEG recordings (data not shown; see [46]). Taking together these findings revealed that conventional estimations of averaged power spectrum mask intrinsic (but stable) segmental structure of electromagnetic field. For example, low alpha-peak in the average spectrum does not suggest that in such EEG (or MEG) there

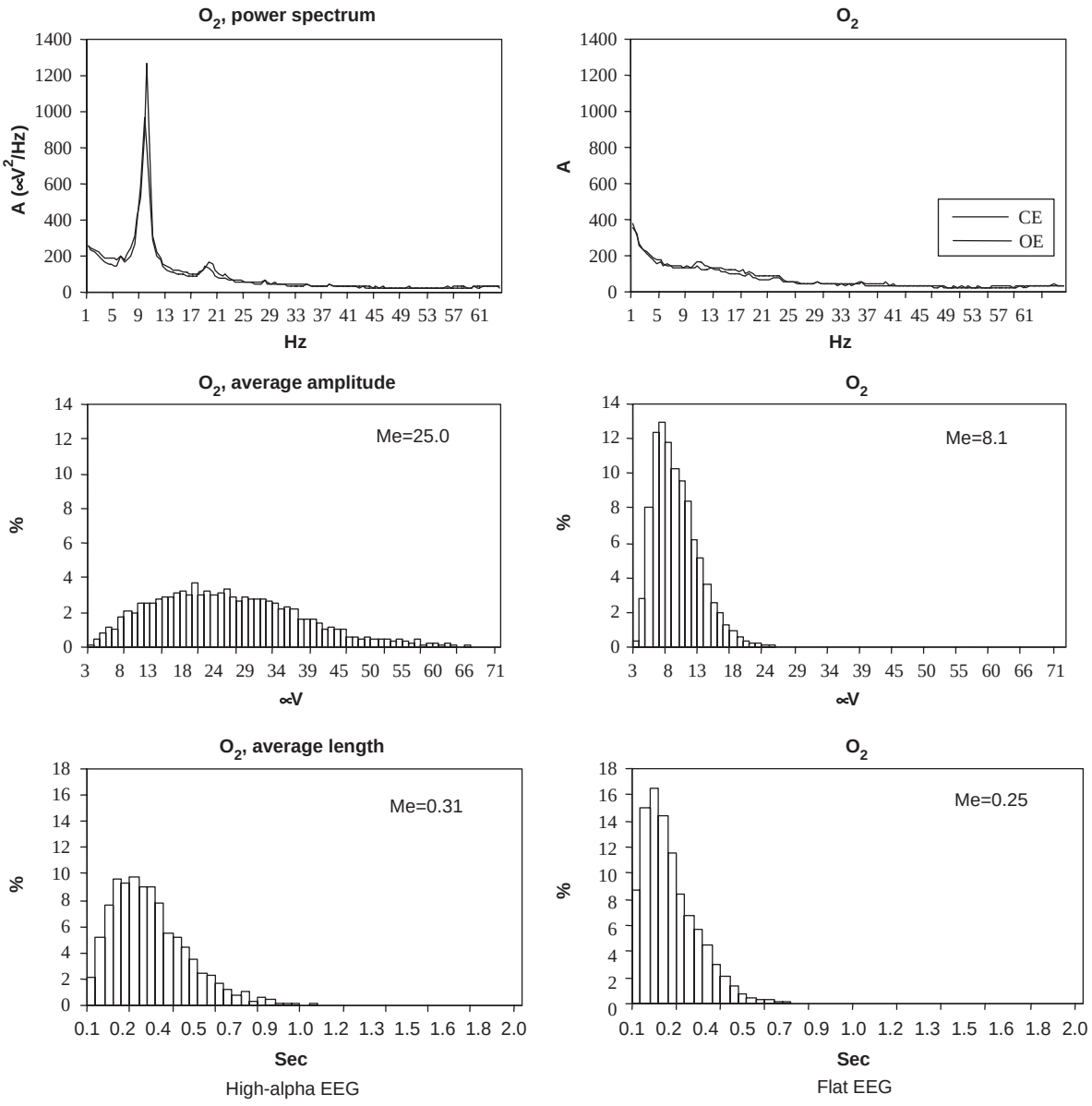

Fig. 4. The distributions of the average ($n = 10$, resting condition) amplitude (A) and length (L) value of EEG segments. Corresponding data are presented separately for "high-alpha" and "flat" EEGs filtered in the alpha frequency band (7–13 Hz). The top row indicates the averaged power spectrum for corresponding EEG types. CE—closed eyes, OE—open eyes, Me—median.

are no high-alpha segments. It is obvious that only relative participation of each segment's amplitude class determines the average level of EEG activity.

Another step in our analysis concerned with the study of the possibility that different EEG/MEG segment attributes may be cross-correlated. Recall that we obtained five segment attributes (A, L, V, AR, S). Together these attributes reflect and permit investigating in detail the intrinsic nature of local (mesolevel) interactions in the neocortex.

Table 1
Pearson correlation coefficients (*rr*) between dynamical series of values of EEG segment attributes

I, Separate channels

	A	L	V	AR	S
A		–	-0.5±0.02	0.79±0.012	–
L	–		–	–	–
V	-0.6±0.02	–		–	–
AR	0.86±0.013	–	–		–
S	–	–	–	–	

F3

II, All channels

	A	L	V	AR
A		0.15±0.1	-0.45±0.02	0.8±0.01
L			–	0.33±0.03
V				0.19±0.1
AR				
S				

O1

Left table illustrates *rr* for separate EEG channels while right table presents *rr* when all EEG channels considered together. The sign ± indicates mean error. *O1*, left occipital EEG electrode; *F3*, left frontal EEG electrode.
A, avarage amplitude within each segment; *L*, average length of segments; *V*, coefficient of amplitude variability within segment *AR*, average amplitude relation among adjacent segments; S, average steepness among adjacebt segments Table modified from Fingelkurts et al. [34] Neuro Image.

To address the question of correlations between segment attributes, Pearson correlation coefficient (*rr*) between dynamical series of values of EEG segment attributes was calculated for each of the EEG location. As an example, the data are shown in Table 1 for eyes-closed-rest-condition for nine subjects (EEG, alpha band). Table 1 (I) illustrates *rr* for two separate EEG channels while Table 1 (II) presents *rr* when all EEG channels ($n = 20$) were considered together.

Significant correlations for two separate EEG channels were observed only for $A \times V$ ($rr = -0.5$, $p < 0.05$) and $A \times AR$ ($rr = 0.79$, $p < 0.05$) segment attributes. Note that average amplitude (A) and average length (L) of segments, as well as other segment attributes were uncorrelated between each other (Table 1, I). These findings testify that majority of the changes of the EEG segment attribute dynamics were determined not by their mutual interrelations, but rather by external factors. Moreover, it permits using each of these segment attributes as an independent index of local operational architectonics of neocortex. It was also demonstrated that obtained peculiarities were very similar qualitatively in different experimental conditions (eyes open and closed, cognitive tasks and pharmacological influence) for both alpha and beta frequency bands (data not shown, see [30,34]).

Each segment attribute has had a particular topological pattern containing 20 components (since there were 20 EEG channels). Therefore, it was interesting to check how similar were the topological patterns of different segment attributes. This analysis is presented on Table 1 II. The topological factor (when all channels were taken into consideration) results in the emergence of significant correlations between almost all segment attributes (Table 1, II). The strongest values of correlation were observed for $A \times AR$ ($rr = 0.8$, $p < 0.05$) and for $AR \times S$ ($rr = 0.76$, $p < 0.05$). At the same time, A and S were uncorrelated between each other. It seems that morpho-functional peculiarities of neocortex determine special conditions, which force similar shifts in pairs of different segment attribute patterns, when topological factor is considered.

As for separate EEG channels, obtained peculiarities for topological patterns of segment attributes were very similar (qualitatively) in different experimental conditions. Taken together, these findings indicate that functional dynamics of neuronal assemblies took place within the rigid and narrow morpho-functional range, which limits temporal (within each location) and topological (between locations) relations between segment attributes. Most likely functional peculiarities of neuronal transient assemblies are reflected in the changes of a particular segment attribute per se along with changes in the functional or cognitive states, rather than in relations between the attributes.

To address the question of functional dynamics of segment attributes, we estimated average values of segment attributes for different EEG amplitude classes. We used amplitude classes since the total averaging of all values within each attribute category has not physiological sense (there are EEG segments with high and low amplitude values). Thus, three amplitude classes were obtained: first and third classes contained 25% of the segments with lowest and highest EEG amplitude correspondingly, while second class contained 50% of the rest of the segments (medium EEG amplitude). EEG was filtered in alpha frequency band (7–13 Hz). In such a way, the segments within these three classes would reflect different degree of local synchronization of cortical neurons within a particular cortex area. Thus, the high amplitude class corresponds to the large neuronal populations, and medium and low amplitude classes correspond to the medium- and small-size neuronal populations correspondingly. Also, some kind of normalization of cortical areas is fulfilled automatically: the local synchronization levels of occipital and frontal areas, for example, have got the same conditions.

It was shown that values of L, AR and S were largest in the low amplitude class and smallest in the medium amplitude class ($p<0.01$). Values of V were largest in the low amplitude class and smallest in the high amplitude class ($0.01<p<0.001$). Although these relations between segment attributes were identical for different experimental conditions, the behavior of individual attributes of different-size neuronal populations was sensitive to the cognitive loading [30] and pharmacological influence [34] as well as to the functional state of the subjects (eyes-open, eyes-closed). Thus, classical effects of ERD/ERS where the ERD during cognitive tasks interpreted as transition from total synchronization of neuronal pools to almost "point" interrelations of neurons [50] may be substantially extended. Obtained findings on the dynamic of neuronal assembly attributes indicate that functional or cognitive loading results not in an elimination of neuronal assemblies, but rather realized in the process of their reorganization into more local and small cell assemblies. Perhaps, such reorganization permits the brain to process the larger amount of operations needed for appropriate cognitive activity. In the framework of this interpretation the periods of ERD and ERS are not the markers of episodes of "active work" and "rest" respectively, but rather are the signs of switching in the dynamic of cortical operations, which are equally active but differing in their processing architecture [51].

Taken together the results of this section showed that segmentation technique permits to study in a precise manner the peculiarities of transient neuronal assemblies' behavior (local interactions in the neocortex), thus allowing to assess the mesolevel of brain description through large-scale measures as an EEG and MEG.

It is obvious that local interaction among neurons and neuronal assemblies (mesolevel) cannot be independent from global integrative processes (macrolevel) in the cortex [17]. To the same conclusion also pointed the fact that topological factor leads to high values of intercorrelation between different segment attributes (see above). This means that segment sequences between different EEG/MEG locations should be temporally synchronized. Such new type of functional interrelations between different cortical areas was called *structural synchrony*, SS (see Methods section).

3.2. Structural synchrony

The estimation of the time-spatial organization of the cortical EEG/MEG is one of the most promising approaches to study the integrative activity of the human brain. Because known approaches inevitably come up against the problem of the nonstationary nature of brain electromagnetic field we have proposed to analyze the functional brain cooperativity by the index of structural synchrony (ISS) which estimates the periods of mutual temporal stabilization of quasi-stationary segments in the multichannel EEG or MEG. Thus, analysis of topological ISS variability would make it possible to trace episodes of the stable cortical inter-area cooperations at the macrolevel independently of partial correlation or coherency.

In order to reveal the functional significance of the proposed ISS, we estimated the behavior of this index in several modeling experiments. In this part of the work we have studied the ISS topological variability in the pairs of EEG channels recorded from longitudinal and transversal electrode arrays. Also the relationship of the ISS versus interelectrode distance was analyzed. Since the topological amplitude maps are varying tremendously between different subjects even during the controlled experimental conditions [52], the data in the present study were collected from the same subjects by numerous repetitions of EEG recording ($n = 24$ for each). Two subjects with well-developed alpha activity participated. Re-testing was conducted after one or two weeks in order to assess temporal stability of obtained effects. EEG was registered from 16 electrodes placed with equal interelectrode distance in two ways: (1) longitudinal array ($n = 16$) placed from O_2 to Fp_2 location (average distance between electrode centers was 1.9 cm) and (2) two transversal arrays ($n = 8$ each) placed frontally from F_8 to F_7 and caudally from T_4 to T_5 location (average distance between electrode centers was 2.9 cm).

Obviously, for short epochs there is a strong likelihood that the two time series, even if entirely independent, will have by chance some degree of synchronicity and this is called the bias [53], so the confidence (stochastic) levels should be calculated for any sample. That is why data from actual EEG was compared with so-called "surrogate" EEG in which a mixing of actual EEG channels was done in such a way that each channel was recorded in a different time. So that, the natural time relations between channels in such EEG were completely destroyed, however, the number and the sequence of segments within each channel remained the same as in the actual EEG. The ISS values obtained from the "surrogate" EEG would thus indicate the relative rate of stochastic alternations (confidence levels) of ISS in the actual EEG.

First of all, it was important to analyze how the level of SS in pairs of EEG channels, taken with equal interelectrode distance, depends from the particular location of each EEG pair on the longitudinal line along the right hemisphere in the posterior-to-anterior direction. This data are presented in Fig. 5. The ISS values for all EEG channel pairs vary from 2.7 to 8.7 and significantly ($p < 0.01 - p < 0.001$, Wilcoxon test) exceeded the level of stochastic synchronization (the 0.4 level). At the same time, despite the fact that all testing pairs had the same interelectrode distance, the average ISS ($n = 48$) exhibited the notable topological picture: it significantly decreased ($p < 0.05$) in a particular location of EEG electrode pair on the head (Fig. 5). However, even the lowest values of ISS were above the stochastic level of synchronization ($p < 0.05$). This data clearly indicate that there are well-outlined cortical areas at the boundaries of which the temporal consistency of segmental architectonics of electrical field became weak. Such findings are in line with conventional approaches where it was also shown that coherence could be quite local and that adjoining pairs, although sharing one site, can be quite different [36].

Fig. 6 presents the data on the topological dynamics of ISS in the two transversal arrays: between right and left lower frontal cortical areas (along the line of standard electrode positions F_8, F_4, F_3 and F_7) and between right and left temporal-parietal cortical areas (along the line of standard electrode positions T_6, P_4, P_3 and T_5).

Obtained data indicate that anterior and posterior brain areas had opposite tendencies in the ISS dynamic. While for the anterior areas the maximal ISS value was detected only for one interhemispheric EEG channels pair (4–5), the same pair showed the minimal ISS value for posterior areas. Here, maximal ISS values in the posterior cortical areas were obtained for homological lateral EEG locations in temporal-parietal areas (Fig. 6). However, these values did not reach statistical significance. Note, that the pairs of homological areas had the similar ISS values. The architecture of callosal axons [54] seems very well fits the obtained results. It was shown that in the anterior part of the brain callosal connections with the same input are very dense near the inter-hemispheric fissure, while in the posterior part the inter-hemispheric fissure is wider and callosal neurons preserve many neighboring connections ipsilaterally along with contralateral ones [55]. A functional interpretation of this fact is that the

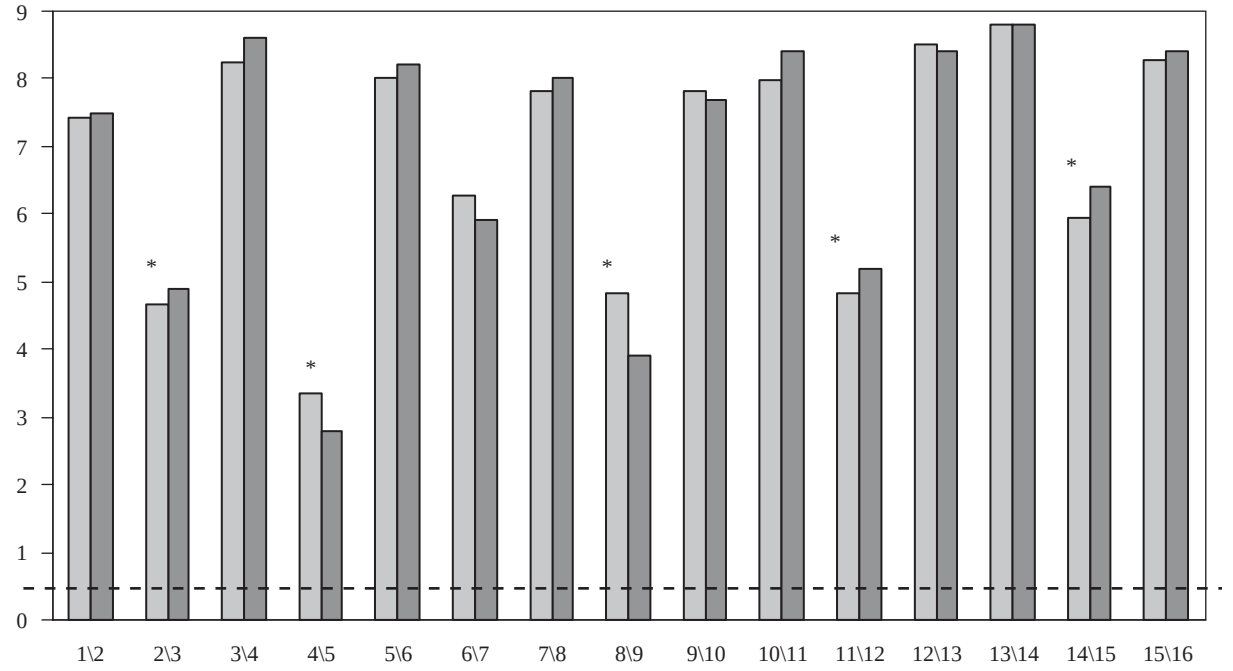

Fig. 5. Mean ISS in the EEG channel pairs, which were located along the longitudinal array of electrodes (posterior-to-anterior), situated on the scalp above the right hemisphere of human brain ($n = 48$). On the horizontal axis the number—label of electrodes, which form pairs of EEG channels, is shown. Pairs 1-2, 5-6, 9-10 and 13-14 correspond to O_2, P_4, C_4 and F_4 electrode positions in standard 10–20 International System. Vertical axis indicates the relative values of ISS. The light and dark histograms correspond to raw and filtered in alpha frequency band EEG correspondingly. Horizontal dotted line shows the maximal level of stochastic ISS for "surrogate" EEG, where different channels are dis-coordinated in time among each other. *Statistically significant ($p < 0.05$, Wilcoxon test) decreasing of ISS in regard with neighboring values.

organization of the frontal regions favors long distance integration and coordination, while posterior regions are more involved in the local processing [35]. It is worth to note, however, that even the lowest values of ISS in our experiment were above the stochastic level of synchronization ($p < 0.05$, Wilcoxon test).

Taken together (Figs. 5 and 6) these findings suggest that ISS (estimated in neighboring EEG pairs) has notable topological peculiarities along the neocortex and thus is sensitive to its morphological and functional organization. Indeed, it is assumed that the cortex is not spatially homogeneous—i.e. is anisotropic [35] and, therefore, ISS values reflect this anisotropy. However, the question whether the ISS depends on the distance between EEG electrode locations is remained. To answer this question, the comparisons of mean values of ISS in pairs of EEG derivations (filtered in the alpha band) as a function of gradually increasing interelectrode distance in longitudinal array of electrodes for posterior-to-anterior direction and vise versa (anterior-to-posterior direction) are presented in Fig. 7.

Based on the volume conduction model, assuming that there is spatial homogeneity in a nonconnected system, one would expect the ISS values to exhibit a smoothed decrement with increased interelectrode distance. Moreover, this decrement should be equal for posterior-to-anterior versus anterior-to-posterior directions. Indeed, we demonstrated that the ISS decreased with the increasing of the interelectrode distance. However, the relationship between the ISS and interelectrode distance was not monotonous: One can see the step-wise dependence with first step-down at the 3.8 cm (1–3 electrodes), second and third steps-down around 9.5 cm (1–6 electrodes)

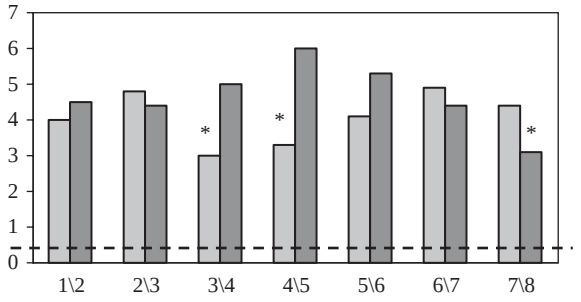

Fig. 6. Mean ISS in the EEG channel pairs, which were located along the two transversal arrays of electrodes (right-to-left), situated on the scalp above anterior (dark histograms) and posterior (light histograms) cortical areas ($n = 48$). On the horizontal axis the number—labels of electrodes, which form pairs of EEG channels are shown. Vertical axis indicates the relative values of ISS. Horizontal dotted line shows the maximal level of stochastic ISS for "surrogate" EEG, where different channels are dis-coordinated in time among each other. *Statistically significant ($p < 0.05$, Wilcoxon test) decreasing of ISS in regard with maximal values of ISS in each array.

and 15.2 cm (1–9 electrodes) correspondently. Previous studies measuring EEG coherence also pointed to a decrease of coherence values with increasing interelectrode distance, however, this dependence was clearly monotonous [36]. Note also that practically all ISS values in our experiment were significantly higher ($p < 0.05 - p < 0.01$ for different pairs, Wilcoxon test) than the stochastic level of synchronization in the "surrogate" EEG (Fig. 7). This notably indicates that even on maximal interelectrode distances there was substantial synchrony between the structural peculiarities of electrical field.

We also found that straight (posterior-to-anterior) and backward (anterior-to-posterior) dependences of ISS from the interelectrode distance were significantly differing between each other. The ISS decreasing for the straight direction was significantly higher ($p < 0.05$) than for the backward direction (Fig. 7). Such so-called "spatial

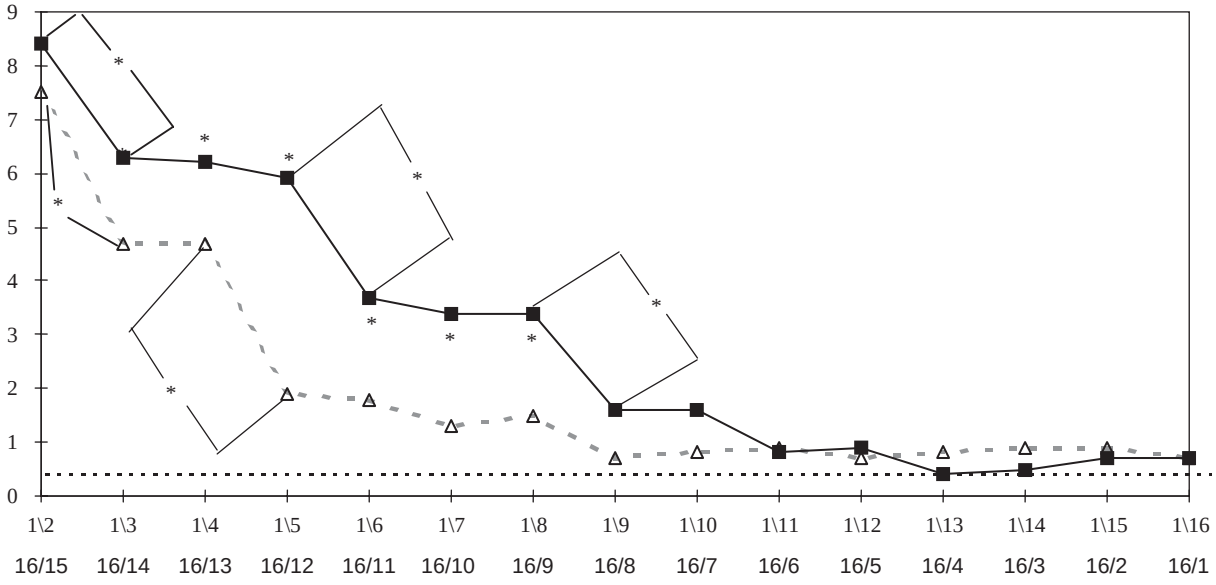

Fig. 7. Mean ISS values in the EEG channel pairs for increasing interelectrode distances in the longitudinal array of electrodes, situated on the scalp above the right hemisphere of human brain ($n = 48$). Dotted line—posterior-to-anterior straight direction—posterior electrodes (1, 2, 3, …), anterior electrodes (…14, 15, 16). Solid line—anterior-to-posterior backward direction. On the horizontal axis the number—label of electrodes, which form pairs of EEG channels are shown. Vertical axis indicates the relative values of ISS. Horizontal dotted line shows the maximal level of stochastic ISS for "surrogate" EEG, where different channels are dis-coordinated in time among each other. *Statistically significant ($p < 0.05$, Wilcoxon test) difference between ISS values in straight and backward dependences and within the same dependence.

hysteresis'', obviously pointed that ISS reflects morpho-functional peculiarities of the different cortical areas and is indicative of a nonisotropic nature of the cortex electrical field, rather than reflects the process of volume conduction of the electrical field in the brain tissue. If ISS would really reflect only volume conduction, changes in the values of ISS should have been equal for the same distances, regardless of which brain areas are involved. Clearly, they were not (see the existence of ''spatial hysteresis'', Fig. 7). This finding is in line with the one described above: Note that the steps in the ISS decreasing (for both directions) coincided with the areas of the cortex where the SS process became weaker (compare Figs. 5 and 6). The hysteresis-like dependence has been extensively documented for coherence analysis also ([35,36,56] among others).

In connection with these findings it was interesting to study the dependence of ISS from the interelectrode distance in the transversal arrays. Initially we supposed that in this way the ''spatial hysteresis'' in the dynamic of ISS from right-to-left and from left-to-right directions would indicate the existence of some sort of interhemispheric asymmetry in the relations of ongoing (without any functional loading) SS processes in the EEG. This data are presented in Fig. 8.

We found that straight (right-to-left) and backward (left-to-right) dependences of ISS did not differ significantly between each other for both transversal arrays along the whole their length (Fig. 8A and B). This finding indicates the absence of notable bilateral asymmetry in the dynamics of ISS in the spontaneous EEG activity, at least in the testing locations. At the same time, it is curious that the ISS decreasing ($p<0.05$) along with increasing of interelectrode distance took place only until forth electrode (8.7 cm) with further stabilization of ISS values until seventh electrode, and increasing ($p<0.05$) of ISS value in the pair of most distant electrodes 1–8 (20.3 cm). These unintuitive for the first sight data are not so surprising if we take into consideration the morphological and functional organization of neocortex. Recall that forth and fifth electrodes were situated on different sides from the interhemispheric fissure, which separates two brain

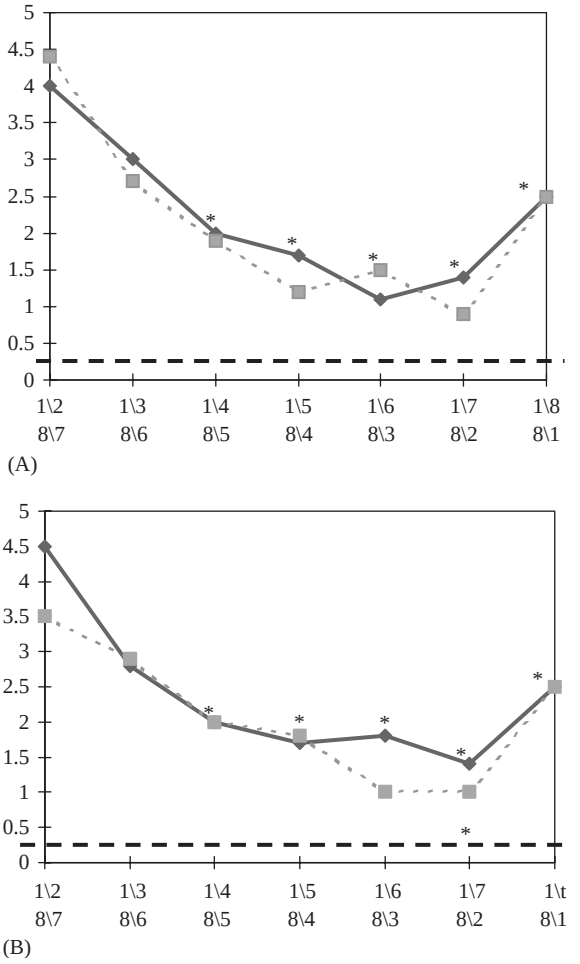

Fig. 8. Mean ISS values ($n=48$) in the EEG channel pairs for increasing interelectrode distances in the transversal arrays of electrodes, situated on the scalp above parietal-temporal cortical areas (A) and frontal cortical areas (B). Solid line—right-to-left direction—right electrodes (1, 2, …), left electrodes (…7, 8). Dotted line—left-to-right direction. On the horizontal axis the number—label of electrodes, which form pairs of EEG channels are shown. Vertical axis indicates the relative values of ISS. Horizontal dotted line shows the maximal level of stochastic ISS for ''surrogate'' EEG, where different channels are dis-coordinated in time among each other. *Statistically significant ($p<0.05$, Wilcoxon test) difference between ISS values in position 1-2 (8-7) and ISS values in all other positions.

hemispheres. So, in contrast to longitudinal array where with increasing distance between EEG electrodes the difference between morpho-functional organization of corresponding cortical areas

also increased, in the case of transversal arrays the morpho-functional differences firstly increase from first till forth electrode (or from eight till fifth), and then decreased reaching its minimum in the most distant, but homologically identical electrode positions 1–8 (F_7–F_8 and T_5–T_6 for frontal and temporal-parietal arrays correspondingly). That is why the ISS in such pairs (with maximal interelectrode distance) exhibited the notably increased values. Anatomical and morphological studies support this finding, pointing that in associative and especially primary cortical areas the callosal connections exist between homological cortical regions [55]. Probably, the ISS has a little dependence from interelectrode distance if these electrodes are situated above homological cortical areas. At least for the posterior array this hypothesis was proved (see Fig. 9). However, for the anterior array the opposite dependence was significant ($p<0.05$). Such differences in the ISS for the anterior and posterior arrays may reflect differences in the morphological and functional organization of the neocortex in these areas. Since the SS process is relatively independent on spectral intensity [22,47], the known differences in EEG spectral intensity between the posterior and anterior regions cannot account for these findings. Also, note that all values of ISS significantly exceeded the stochastic level of synchronization in the "surrogate" EEG (Fig. 9).

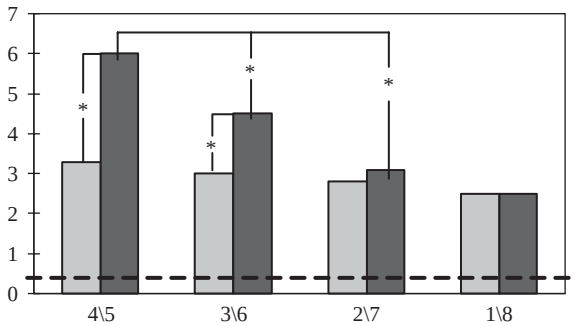

Fig. 9. Mean ISS values ($n=48$) in the EEG channel pairs registered from symmetrical cortical areas in anterior (dark histograms) and posterior (light histograms) transversal electrode arrays. On the horizontal axis the number—label of electrodes, which form pairs of EEG channels are shown. Vertical axis indicates the relative values of ISS. Horizontal dotted line shows the maximal level of stochastic ISS for "surrogate" EEG, where different channels are dis-coordinated in time among each other. *Statistically significant ($p<0.05$, Wilcoxon test) difference between ISS values in a tested position.

Thus, our analysis of the results of modeling experiments strongly pointed that ISS is sensitive to morpho-functional organization of the neocortex, resulting in higher values of structural synchrony between cortical areas which are homological and, thus, most likely participating in the same functional acts. However, the distance between these areas has its contribution to the ISS also.

More generally, these findings suggest the existence of statistical heterogeneity (anisotropy) of electromagnetic field in regard to the processes of mutual stabilizations of regional EEGs and/or MEGs. These conclusions get more evidence power considering that the subjects underwent the same experiment with the same conditions twice. The test–retest reliabilities of the obtained ISS values between the two sessions (obtained through 1–2 weeks) were very high what confirmed the reliabilities of the findings. The test–retest reliabilities minimize both Type I and Type II errors because by definition chance findings do not replicate [57].

Most likely, the topological peculiarities of SS phenomenon obtained in the described study are related with well established already in the classical work of Motokawa (1944, cited in [58]) fact on the spatial heterogeneity of neocortex, measuring by crosscorrelation. Later this fact has got considerable support [35,56,58]. Although there are several fundamental investigations of crosscorrelation and coherency relations in longitudinal and transversal arrays of EEG electrodes [35,36,56,58], for us it was important to obtain crosscorrelation coefficients exactly from the same EEG registrations, since we wanted to make precise comparisons between SS and crosscorrelation approaches.

3.3. Comparisons of SS index and Pearson correlation coefficient

In order to compare the results of proposed approach of structural synchrony (SS) with some of conventional methods, the Pearson coefficients

of correlation (rr) were calculated for the same data. However, the segment metaphor of EEG architectonic demands more accurate estimation of rr than it is usually done. Thus, the rr were calculated for consecutive short segments of EEG by means of sliding window (256 data-points = 2 s). This size of window was chosen since it is well established that EEG signal is relatively stationary within 2 s (for the discussion see [59,60]. The crosscorrelation function on the zero shift (rr_0) and the maximum value of this function (rr_{max}) were estimated in each window. The resulted values ($n = 30$ for each EEG) of rr_0 and rr_{max} were obtained as average values of rr for all windows in each EEG recording. The time shift of correlation function for rr_{max} is not analyzed in this work, since for the purposes of the present analysis it was important to compare the values of rr_0 and rr_{max} (see below). All operations with rr were done after the normalization procedure using the Fisher z-transformations:

$$z = 0.5 \ln \frac{1+r}{1-r}, \text{ where } r \text{ is the } rr \text{ value.}$$

The hypothesis about no differences between two samples of rr were checked using statistics λ, which has near normal distribution:

$$\lambda = \frac{|z1 - z2|}{\sqrt{(1/n1 - 3) + (1/n2 - 3)}},$$

where $z1$ and $z2$ are z-estimations of rr testing, $n1-3$ and $n2-3$ the degree of freedom for corresponding samples.

Table 2 presents the values of rr_0 and rr_{max} in pairs of neighboring EEG channels in the longitudinal array (posterior-to-anterior direction). Three pairs (4–5, 8–9 and 11–12) exhibited significant decrease of rr_0 values in regard to the majority rr_0. Similar tendency was observed in the dynamic of 2–3 and 14–15 EEG pairs (Table 2). Obtained decreasing in rr_0 values, however, was not related to the phase shift of EEG rhythmic component since almost in all cases the values of rr_0 and rr_{max} coincided between each other.

Although the results of crosscorrelation analysis (Table 2) and analogous data for ISS (Fig. 5) were similar, the SS description of interrelations between cortical areas was more contrast and pronounced. The same rule was found when the interelectrode distance was taken into consideration (Table 3). The rr values decreased more

Table 2
The rr_0 and rr_{max} values in neighboring EEG channel pairs in the longitudinal array (posterior-to-anterior) of electrodes (for details see Fig. 5)

Pairs	rr_0	rr_{max}	p
1–2	0.99	0.99	—
2–3	0.94	0.95	—
3–4	1.00	1.00	—
4–5	0.83	0.88	**
5–6	0.99	0.99	—
6–7	0.97	0.97	—
7–8	0.99	0.99	—
8–9	0.92	0.91	**
9–10	0.99	0.99	—
10–11	0.99	0.99	—
11–12	0.95	0.95	*
12–13	0.99	0.99	—
13–14	0.99	0.99	—
14–15	0.96	0.96	—
15–16	0.99	0.99	—

*$p<0.05$, **$p<0.01$ statistically significant (Wilcoxon test) decrease of rr_0 and rr_{max} in regard with the neighboring values.

Table 3
Mean rr_0 and rr_{max} values for increasing interelectrode distances in the longitudinal array (posterior-to-anterior versus anterior-to-posterior) of EEG electrodes (for details see Fig. 7)

Pairs	rr_0 (p-to-a)	rr_0 (a-to-p)	P	rr_{max} (p-to-a)	rr_{max} (a-to-p)	P
1–2	0.99	0.99	—	0.99	0.99	—
1–3	0.95	0.96	—	0.95	0.96	—
1–4	0.95	0.95	—	0.95	0.95	—
1–5	0.68	0.95	**	0.78	0.95	**
1–6	0.65	0.86	**	0.76	0.86	*
1–7	0.55	0.86	**	0.67	0.86	**
1–8	0.50	0.83	**	0.65	0.83	**
1–9	0.21	0.64	***	0.51	0.66	*
1–10	0.16	0.61	***	0.49	0.65	*
1–11	0.13	0.50	***	0.49	0.57	*
1–12	−0.01	0.47	***	0.45	0.57	*
1–13	−0.02	0.07	—	0.45	0.44	—
1–14	−0.01	0.07	—	0.45	0.44	—
1–15	−0.06	−0.05	—	0.44	0.43	—
1–16	−0.06	−0.06	—	0.43	0.43	—

*$p<0.05$, **$p<0.01$, ***$p<0.001$, statistically significant (Wilcoxon test) decrease of rr_0 and rr_{max} in regard with array edge values.

Table 4
Mean rr_0 and rr_{max} values in neighboring EEG channel pairs in the transversal arrays (right-to-left) of electrodes in posterior and anterior parts of cortex (for details see Fig. 6)

Pairs	Posterior	Anterior	p
1–2	0.91	0.92	—
2–3	0.93	0.95	—
3–4	0.88	0.95	**
4–5	0.87	0.98	***
5–6	0.92	0.95	**
6–7	0.95	0.93	—
7–8	0.91	0.88	—

*$p<0.05$, **$p<0.01$, ***$p<0.001$, statistically significant (Wilcoxon test) differences of rr between the same electrode pairs taken for different arrays.

Table 5
Mean rr_0 and rr_{max} values for increasing interelectrode distances in two transversal EEG arrays (for details see Fig. 8)

Pairs	rr_0		rr_{max}	
	Posterior	Anterior	Posterior	Anterior
1–2	0.91	0.92	0.91	0.92
1–3	0.87	0.84	0.87	0.84
1–4	0.72	0.75	0.73	0.75
1–5	0.61	0.69	0.62	0.69
1–6	0.55	0.64	0.56	0.64
1–7	0.48	0.57	0.51	0.57
1–8	0.43	0.50	0.46	0.50

Here the statistically significant level ($p<0.05$) for rr was equal to 0.21. The dispersion for averaged rr values did not exceed 0.007.

strongly for straight (posterior-to-anterior) dependence than for backward (anterior-to-posterior) dependence. Here also the phase shift was not the main factor since the decrease in rr values was similar for rr_0 and rr_{max}. However, the fall of rr values (Table 3) was much more monotonous than the decrease in ISS values (Fig. 7).

The dynamic of rr_0 for pairs of EEG channels in transverse arrays also repeated the dynamics of analogues data for ISS (Table 4), but in a much more monotonous way. Similar monotonous dependence, but for coherence values was also found [36].

Obtained similarity (at least for the high-alpha EEG) in the two principally different approaches for estimation of the functional relations between cortical areas, probably, reflects the fact that both approaches are sensitive to the same basic characteristic of bioelectrical field. However, since the ISS values were more contrast in detecting the nonhomogeneity of this field, most likely exactly the temporal synchrony between segmental structures of local EEG determines the estimated values of rr_{max} between them. Indeed, when alpha activity is well developed, the highest phase stabilization is observed within alpha-spindles [61]. The rapid transition periods (RTP) also more frequently located in the beginning and the end of alpha-spindles in the case of well developed alpha activity [62]. Thus, the more frequent and precise is the temporal synchronization of these alpha-spindle segments (or other quasi-stationary segments) in two signals, the higher would be the maximal average values of crosscorrelation function. Considering a well-known high degree of comparability between correlation and coherence analyses under normal physiological conditions, we may predict that the same relation would be valid also for the coherence measure (Coh).

Therefore, findings of the present study enable us to conclude that temporal consistency of EEG segmental structure initially underlies and determines the high values of rr (and coherency). However, in the case of less structured architectonics of electromagnetic field and during cognitive tasks, the dynamic characteristics of SS and rr (Coh) indices may substantially mismatch [51]. The data obtained from transversal arrays, where interelectrode distance was taken into consideration, support this supposition (Table 5). Since the alpha activity was not pronounced in the temporal and low frontal areas, the dynamic of ISS and rr values were notably different in these areas. The rr values decreased monotonically along whole array distance (Table 5) while the ISS values significantly increased in the pair of the most distant, but functionally homologies EEG electrodes (Fig. 8), thus indicating that ISS in contrast to rr is more sensitive to morpho-functional peculiarities of the neocortex. This interpretation is also supported by cognitive studies demonstrating an opposite tendencies in rr and ISS values during cognitive

loading [51]. For example, the *rr* values decreased during arithmetic counting when compared with the rest state, while the ISS values increased. Also the topology of connected cortical areas was differing for crosscorrelation and structural synchrony approaches [51].

3.4. Application of segmental and SS methods

The application of the segmental and SS methods for EEG/MEG signal analysis in neurophysiological studies demonstrated their sufficiently high sensitivity in estimation of the EEG/MEG segments and synchrony dynamics related to different functional states of subjects [22], sleep stages [63], cognitive and memory processing [47], pharmacological influences [34,44], multisensory integration [46], and in psychiatry [51].

4. Concluding remarks

Among the many electro- and magneto-physiological signals of the human organism encountered in basic and clinical research, the EEG (and MEG) has the most of nonstationary behavior. Indeed, EEG/MEG signals have been shown to have nonstationary behavior in a variety of contexts [33,47,64]. From a theoretical point of view, the activity of neuronal assemblies (as nonlinear dynamic systems) should inevitably be nonstationary since it reflects the different stages of a self-organized process [8,10]. At the same time, the phenomenology of the EEG/MEG signal shows that it can be presented as a sequence of quasi-stationary segments, which are separated by the rapid transitive processes [65] (for the reviews, see [14,21,22,24]).

In the present paper we observed the novel methodology for the piecewise analysis of EEG/MEG signal (SECTION 01®). This approach segments the EEG/MEG signal and simultaneously identifies the five quantitative attributes for each EEG/MEG segment. We supposed that in these segments the quasi-stable activity of neuronal assemblies are reflected. The analysis presented in this paper suggests that it may have important usage to identify physiological components that retain their identity despite the inter-subject EEG/MEG substantial variability. Such results are not possible with conventional methods of EEG/MEG analysis because they are not sensitive to the underlining quasi-stationary nature of the signals.

If EEG/MEG segments are real local phenomena, then it is possible to suppose that between such segments there should be a certain functional connection. This supposition has leaded us to develop a new methodology for identifying functional connectivity in the multichannel EEG/MEG signal (JUMPSYN 01®): Estimation of coincidences of the boundaries between quasi-stationary EEG/MEG segments. With this methodology we have discovered a new type of integrative brain activity—structural synchrony (SS). It is important to note that in the case of SS processes, it is not the immediate amplitudes of the signal in the EEG/MEG pairs and their rhythmical components, but the moments of shifting of quasi-stationary EEG/MEG segments among different channels that are synchronized. This type of synchrony reflects a true functional connectivity between different brain areas by means of coupled operations (for a discussion, see [43]). It seems that this hypothesis is consistent with Friston's conception about two different types of synchrony [66]: synchronous cortex connectivity (like correlation, coherency etc.), and asynchronous coupling as nonlinear interaction between neuronal populations or assemblies. Most likely, discovered by us structural synchrony is an explicit characteristic of such nonlinear type of cortex functional integration.

Even though, much more research is needed to study further the behavior of local and remote structural synchrony during different brain functional and pathological states, the capacity of SECTION 01® and JUMPSYN 01® technologies to reveal the EEG/MEG structure (in terms of segments and structural synchrony) is apparent. These technologies made it possible to develop new insights regarding the time structure of EEG/MEG and provide practical indexes which can serve as additional diagnostic markers of some brain and psychiatric disorders [67]. Further work is needed to determine the generality of these findings and to test the hypothesis that there are

different time-scales on which structural descriptions of EEG/MEG can be done. This would be a major step towards a better understanding of the functional organization of the neocortex.

Acknowledgments

The authors wish to thank Dr. Boris Brodsky, Dipl. Med. Eng. Viktor Ermolaev and IT specialist Carlos Neves for software development and technical support. Different parts of this work have been funded by the Russian Fund of Basic Research (96-04-49144; Russia), Russian Universities Foundation–Basic Research (11-3653; Russia), CIMO Foundation (Finland), and BM-SCIENCE funds (Finland). Authors want to express special gratitude to Dr. Sergei Shishkin, Prof. Paul Nunez, Prof. Ben Jansen, and Prof. Dietrich Lehmann who the basic ideas and results of the present work were at various times discussed with.

References

[1] G. Rose, M. Siebler, Cooperative effects of neuronal ensembles, Exp. Brain Res. 106 (1995) 106–110.
[2] Y.I. Arshavsky, Cellular and network properties in the functioning of the nervous system: from central pattern generators to cognition, Brain Res. Brain Res. Rev. 41 (2003) 229–267.
[3] P.L. Nunez, Neocortical dynamics of macroscopic-scale EEG measurements, IEEE Eng. Med. Biol. Mag. 17 (1998) 110–117.
[4] S.L. Bressler, J.A.S. Keslo, Cortical coordination dynamics and cognition, Trends Cogn. Sci. 5 (2001) 26–36.
[5] O. David, D. Cosmelli, K.L. Friston, Evaluation of different measures of functional connectivity using a neural mass model, Neuroimage 21 (2004) 659–673.
[6] M. Bezzi, M.E. Diamond, A. Treves, Redundancy and synergy arising from pairwise correlations in neuronal ensembles, J. Comput. Neurosci. 12 (2002) 165–174.
[7] P. Kudela, P.J. Franaszczuk, G.K. Bergey, Changing excitation and inhibition in simulated neural networks: effects on induced bursting behavior, Biol. Cybern. 88 (2003) 276–285.
[8] W.J. Freeman, Evidence from human scalp electroencephalograms of global chaotic itinerancy, Chaos 13 (2003) 1067–1077.
[9] M.W. Slutzky, P. Cvitanovic, D.J. Mogul, Identification of determinism in noisy neuronal systems, J. Neurosci. Methods 118 (2002) 153–161.
[10] G. Schoner, J.A. Kelso, Dynamic pattern generation in behavioral and neural systems, Science 239 (1988) 1513–1520.
[11] K.J. Friston, Transients, metastability, and neuronal dynamics, Neuroimage 5 (1997) 164–171.
[12] An.A. Fingelkurts, Al.A. Fingelkurts, Making complexity simpler: multivariability and metastability in the brain, Int. J. Neurosci. 114 (2004) 843–862.
[13] J.A.S. Kelso, Review of Dynamic Patterns: The Self-Organization of Brain and Behavior, MIT Press, Cambridge, MA, 1995.
[14] A.Ya. Kaplan, Nonstationary EEG: methodological and experimental analysis, Usp. Physiol. Nauk (Success in Physiological Sciences) 29 (1998) 35–55 (in Russian).
[15] E. Basar, M. Özgören, S. Karakas, C. Basar-Eroglu, Super-synergy in the brain: The grandmother percept is manifested by multiple oscillations, Int. J. Bifurcat. Chaos 14 (2004) 453–491.
[16] W. Klimesch, Event-related band power changes and memory performance, in: G. Pfurtscheller, F.H. Lopez da Silva (Eds.), Event-Related Desynchronization. Handbook of Electroencephalography and Clinical Neurophysiology, Elsevier, Amsterdam, 1999, pp. 161–178.
[17] P.L. Nunez, Toward a quantitative description of large-scale neocortical dynamic function and EEG, Behav. Brain Sci. 23 (2000) 371–437.
[18] A. Effern, K. Lehnertz, G. Fernandez, T. Grunwald, P. David, C.E. Elger, Single trial analysis of event related potentials: non-linear de-noising with wavelets, Clin. Neurophysiol. 111 (2000) 2255–2263.
[19] Al.A. Fingelkurts, An.A. Fingelkurts, C.M. Krause, M. Sams, Probability interrelations between pre-/post-stimulus intervals and ERD/ERS during a memory task, Clin. Neurophysiol. 113 (2002) 826–843.
[20] N.A. Laskaris, A.A. Ioannides, Exploratory data analysis of evoked response single trials based on minimal spanning tree, Clin. Neurophysiol. 112 (2001) 698–712.
[21] An.A. Fingelkurts, Al.A. Fingelkurts, Operational architectonics of the human brain biopotential field: Towards solving the mind-brain problem, Brain Mind 2 (2001) 261–296.
[22] A.Ya. Kaplan, S.L. Shishkin, Application of the change-point analysis to the investigation of the brain's electrical activity, in: B.E. Brodsky, B.S. Darkhovsky (Eds.), Non-parametric Statistical Diagnosis. Problems and Methods, Kluwer Acad Publ., Dordrecht, 2000, pp. 333–388.
[23] An.A. Fingelkurts, Al.A. Fingelkurts, Operational architectonics of perception and cognition: A principle of self-organized metastable brain states, VI Parmenides workshop—Perception and thinking, Institute of Medical Psychology, April 5–10, Elba/Italy (invited full-text contribution), 2003, URL = http://www.bm-science.com/team/art24.pdf.
[24] J.S. Barlow, Methods of analysis of nonstationary EEGs, with empahasis on segmentation techniques: A comparative review, J. Clin. Neurophysiol. 2 (1985) 267–304.

[25] D. Lehmann, H. Ozaki, I. Pal, EEG alpha map series: Brain micro-states by space oriented adaptive segmentation, Electroencephalogr. Clin. Neurophysiol. 67 (1987) 271–288.
[26] H.M. Praetorius, G. Bodenstein, O.D. Creutzfeldt, Adaptive segmentation of EEG records: a new approach to automatic EEG analysis, Electroencephalogr. Clin. Neurophysiol. 42 (1977) 84–94.
[27] B.H. Jansen, A. Hasman, R. Lenten, S.L. Visser, Usefulness of autoregressive models to classify EEG-segments, Biomed. Tech. (Berl). 24 (1979) 216–223.
[28] A.Ya. Kaplan, An.A. Fingelkurts, Al.A. Fingelkurts, S.L. Shishkin, R.M. Ivashko, Spatial synchrony of human EEG segmental structure, Zh. Vyssh. Nerv. Deiat. Im. I.P. Pavlova (I.P. Pavlova J. Higher Nerve Activity) 50 (2000) 624–637 (in Russian).
[29] B.E. Brodsky, B.S. Darkhovsky, A.Ya. Kaplan, S.L. Shishkin, A nonparametric method for the segmentation of the EEG, Comput. Methods Progams. Biomed. 60 (1999) 93–106.
[30] A.Ya. Kaplan, S.V. Borisov, Dynamic properties of segmental characteristics of EEG alpha activity in rest conditions and during cognitive tasks, Zh. Vyssh. Nerv. Deiat Im. I.P. Pavlova (I.P. Pavlov J. Higher Nervous Activity) 53 (2003) 22–31 (in Russian).
[31] A.Ya. Kaplan, Al.A. Fingelkurts, An.A. Fingelkurts, B.S. Darkhovsky, Topological mapping of sharp reorganization synchrony in multichannel EEG, Am. J. END Technol. 37 (1997) 265–275.
[32] J. Fell, A. Kaplan, B. Darkhovsky, J. Röschke, EEG analysis with nonlinear deterministic and stochastic methods: a combined strategy, Acta Neurobiol. Exp. 60 (2000) 87–108.
[33] W.A. Truccolo, M. Ding, K.H. Knuth, R. Nakamura, S. Bressler, Trial-to-trial variability of cortical evoked responses: Implications for analysis of functional connectivity, Clin. Neurophysiol. 113 (2002) 206–226.
[34] An.A. Fingelkurts, Al.A. Fingelkurts, R. Kivisaari, E. Pekkonen, R.J. Ilmoniemi, S.A. Kähkönen, Local and remote functional connectivity of neocortex under the inhibition influence, Neuroimage 22 (2004) 1390–1406.
[35] R.W. Thatcher, P.J. Krause, M. Hrybyk, Cortico-cortical associations and EEG coherence: a two-compartmental model, Electroencephalogr. Clin. Neurophysiol. 64 (1986) 123–143.
[36] T.H. Bullock, M.C. McClune, J.Z. Achimowicz, V.J. Iragui-Madoz, R.B. Duckrow, S.S. Spencer, EEG coherence has structure in the millimeter domain: subdural and hippocampal recordings from epileptic patients, Electroencephalogr. Clin. Neurophysiol. 95 (1995) 161–177.
[37] J.C. Shaw, D. Simpson, EEG coherence: Caution and cognition, Br. Psychophysiol. Soc. Q. 30–31 (1996–1997) 7–9.
[38] J.C. Shaw, Correlation and coherence analysis of the EEG: a selective totorial review, Int. J. Psychophysiol. 1 (1984) 255–266.
[39] L.A. Baccala, K. Sameshima, Partial directed coherence: a new concept in neural structure determination, Biol. Cybern. 84 (2001) 463–474.
[40] J. Gross, M. Kujala, M. Hämäläinen, L. Timmermann, A. Schnitzler, R. Salmelin, Dynamic imaging of coherent sources: Studying neural interactions in the human brain, Proc. Natl. Acad. Sci. USA 98 (2001) 694–699.
[41] K.J. Friston, C. Buchel, Attentional modulation of effective connectivity from V2 to V5/MT in humans, Proc. Natl. Acad. Sci. USA 97 (2000) 7591–7596.
[42] P.A. Tass, Phase Resetting in Medicine and Biology, Springer, Berlin, 1999, pp. 247–248.
[43] An.A. Fingelkurts, Al.A. Fingelkurts, S. Kähkönen, Functional connectivity in the brain—is it an elusive concept?, Neurosci. Biobehav. Rev. 28 (2005) 827–836.
[44] An.A. Fingelkurts, Al.A. Fingelkurts, R. Kivisaari, E. Pekkonen, R.J. Ilmoniemi, S.A. Kähkönen, Enhancement of GABA-related signalling is associated with increase of functional connectivity in human cortex, Human Brain Mapp. 22 (2004) 27–39.
[45] E. Bullmore, C. Long, J. Suckling, J. Fadili, G. Calvert, F. Zelaya, T.A. Carpenter, M. Brammer, Colored noise and computational inference in neurophysiological (fMRI) time series analysis: resampling methods in time and wavelet domains, Hum. Brain Mapp. 12 (2001) 61–78.
[46] An.A. Fingelkurts, Al.A. Fingelkurts, C.M. Krause, R. Möttönen, M. Sams, Cortical operational synchrony during audio-visual speech integration, Brain Language 85 (2003) 297–312.
[47] An.A. Fingelkurts, Al.A. Fingelkurts, C.M. Krause, A.Ya. Kaplan, S.V. Borisov, M. Sams, Structural (operational) synchrony of EEG alpha activity during an auditory memory task, NeuroImage 20 (2003) 529–542.
[48] S.L. Shishkin, B.E. Brodsky, B.S. Darkhovsky, A.Ya. Kaplan, EEG as a non-stationary signal: an approach to analysis based on non-parametric statistics, Human Physiol. (Fiziol. Cheloveka) 23 (1997) 124–126 (in Russian).
[49] S.L. Shishkin, B.S. Darkhovsky, Al.A. Fingelkurts, An.A. Fingelkurts, A.Ya. Kaplan, Interhemisphere synchrony of short-term variations in human EEG alpha power correlates with self-estimates of functional state, In Proceedings of the Ninth World Congress of Psychophysiology, Italy, Tvaormin, Sicily, 1998, p. 133.
[50] G. Pfurtscheller, F.H. Lopes da Silva, Event-related EEG/MEG synchronization and desynchronization: basic principles, Clin. Neurophysiol. 110 (1999) 1842–1857.
[51] S.V. Borisov, Studying of a phasic structure of the alpha activity of human EEG, Ph.D. Thesis, Moscow State University, 2002, p. 213 (in Russian).
[52] A.P. Burgess, J. Gruzelier, How reproducible is the topographical distribution of EEG amplitude?, Int. J. Psychophysiol. 26 (1997) 113–119.
[53] T.H. Bullock, Signals and signs in the nervous system: The dynamic anatomy of electrical activity, Proc. Natl. Acad. Sci. USA 94 (1997) 1–6.

[54] H. Kennedy, C. Meissirel, C. Dehay, Callosal pathways and their compliancy to general rules governing the organization of corticocortical connectivity, in: B. Dreher, S.R. Robinson (Eds.), Vision and Visual Dysfunction, Vol. 3, McMillan Press, London, 1991, pp. 324–359.

[55] G. Berlucchi, Recent advances in the analysis of the neural substrate of interhemispheric communication, in: O. Pompeiano, C. Ajmone Marsan (Eds.), Brain Mechanisms and Perceptual Awareness, Raven Press, New York, 1981, pp. 133–152.

[56] H. Ozaki, H. Suzuki, Transverse relationships of the alpha rhythm on the scalp, Electroencephalogr. Clin. Neurophysiol. 66 (1986) 191–195.

[57] F. Duffy, J.R. Hughes, F. Miranda, P. Bernard, P. Cook, Status of quantitative EEG (QEEG) in clinical practice, Clin. Electroencephalogr. 25 (1994) VI–XXII.

[58] H. Hori, K. Hayasaka, K. Sato, O. Harada, H. Iwata, A study on phase relationship in human alpha activity. Correlation of different regions, Electroencephalogr. Clin. Neurophysiol. 26 (1969) 19–24.

[59] O.D. Creutzfeldt, G. Bodenstein, J.S. Barlow, Computerized EEG pattern classification by adaptive segmentation and probability density function classification: clinical evaluation, Electroenceph. Clin. Neurophysiol. 60 (1985) 373–393.

[60] T. Inouye, S. Toi, Y. Matsumoto, A new segmentation method of electroencephalograms by use of Akaike's information criterion, Brain Res. Cogn. Brain Res. 3 (1995) 10–33.

[61] R.B. Levine, R.P. Smith, G.R. Hawkes, On synchrony of the alpha rhythms, Aerosp. Med. 34 (1963) 349–352.

[62] An.A. Fingelkurts, Time-spatial organization of human EEG segment's structure, Ph.D. Thesis, Moscow State University, 1998, p. 415 (in Russian).

[63] A. Kaplan, J. Roschke, B. Darkhovsky, J. Fell, Macrostructural EEG characterization based on nonparametric change point segmentation: application to sleep analysis, J. Neurosci. Methods 106 (2001) 81–90.

[64] M.P. Tarvainen, J.K. Hiltunen, P.O. Ranta-Aho, P.A. Karjalainen, Estimation of nonstationary EEG with Kalman smoother approach: an application to event-related synchronization (ERS), IEEE Trans. Biomed. Eng. 51 (2004) 516–524.

[65] G. Bodenstein, H.M. Praetorius, Feature extraction from the electroencephalogram by adaptive segmentation, Proc. IEEE 65 (1977) 642–652.

[66] K.J. Friston, The labile brain. I. Neuronal transients and nonlinear coupling, Philos. Trans. Roy. Soc. London Ser. B 355 (2000) 215–236.

[67] An.A. Fingelkurts, Al.A. Fingelkurts, S. Kähkönen, New perspectives in pharmaco-electroencephalography, Prog. Neuropsychopharm. Biol. Psychiatry 29 (2005) 193–199.

[68] D. Lehmann, EEG assessment of brain activity: spatial aspects, segmentation and imaging, Int. J. Psychophysiol. 1 (1984) 267–276.